Cover Page

Title: *GIGANTEA* Is A Negative Regulator Of Abscisic Acid Transcriptional Responses And Sensitivity In Arabidopsis

Running head: *GIGANTEA* suppresses abscisic acid responses

Corresponding author: L. Conti; Dipartimento di Bioscienze, Università degli studi di Milano/ Via Celoria 26 /Milano / 20133/ Italy/ 0039 0250315012/ Lucio.Conti@unimi.it

Subject areas: environmental and stress responses, regulation of gene expression

Number of:

- **black and white figures :** 0
- **colour figures:** 5
- **tables:** 0

Type and number of supplementary materials: 9 Supplementary Figures, 6 Supplementary tables

Title Page

Title: *GIGANTEA* is a negative regulator of abscisic acid transcriptional responses and sensitivity in Arabidopsis

Running head: *GIGANTEA* suppresses abscisic acid responses

Authors

Beata Siemiatkowska[1§], Matteo Chiara[1§], Bhaskara G. Badiger[2], Matteo Riboni[1], Francesca D'Avila[3], Daniele Braga[3#], Mohamed Abd Allah Salem[4], Damiano Martignago[1], Sara Colanero[1], Massimo Galbiati [5], Patrick Giavalisco[6], Chiara Tonelli[1], Thomas E. Juenger[2] and Lucio Conti[1*]

Affiliations

[1] = Dipartimento di Bioscienze, Università degli Studi di Milano, Italy

[2] = Department of Integrative Biology, The University of Texas at Austin, USA

[3] = Dipartimento di Scienze della Salute, Università degli Studi di Milano, Italy

[4] = Department of Pharmacognosy, Faculty of Pharmacy, Menoufia University, Egypt

[5] = Istituto di Biologia e Biotecnologia Agraria – IBBA, CNR – Milano, Italy

[6] = Max Planck Institute for Biology of Ageing, Cologne, Germany

[#] = Present address IRCCS Humanitas Clinical and Research Center, Rozzano, MI, Italy

§ = equal contribution

* Lucio.Conti@unimi.it

Abstract

Transcriptional reprogramming plays a key role in drought stress responses, preceding the onset of morphological and physiological acclimation. The best-characterised signal regulating gene expression in response to drought is the phytohormone abscisic acid (ABA). ABA-regulated gene expression, biosynthesis and signalling are highly organised in a diurnal cycle, so that ABA-regulated physiological traits occur at the appropriate time of the day. The mechanisms that underpin such diel oscillations in ABA signals are poorly characterised. Here we uncover *GIGANTEA* (*GI*) as a key gatekeeper of ABA-regulated transcriptional and physiological responses. Time-resolved gene expression profiling by RNA sequencing under different irrigation scenarios indicates that *gi* mutants produce an exaggerated ABA response, despite accumulating wild-type levels of ABA. Comparisons with ABA-deficient mutants confirm the role of GI in controlling ABA-regulated genes and the analysis of leaf temperature, a read-out for transpiration, supports a role for GI in the control of ABA-regulated physiological processes. Promoter regions of GI/ABA-regulated transcripts are directly targeted by different classes of transcription factors, especially PHYTOCHROME-INTERACTING FACTORs, and (ABRE)-BINDING FACTOR, together with GI itself. We propose a model whereby diel changes in GI control oscillations in ABA responses. Peak GI accumulation at midday contributes to establishing a phase of reduced ABA sensitivity and related physiological responses, by gating DNA binding or function of different classes of transcription factors that cooperate or compete with GI at target regions.

Keywords

Arabidopsis thaliana, Circadian rhythms, Drought stress. Transcription factors

Introduction

Several drought responses rely on short term transcriptional reprogramming of physiological and metabolic-related genes to enable long term morphological adjustments. These gene regulatory events respond to combinations of signals to allow precise spatial/temporal organization. As these signals converge to chromatin regions, one key question is to understand what mechanisms enable their transduction and integration onto regulatory DNA sequences, as this would allow a better understanding of the evolution of adaptive strategies in response to water deficit.

The best characterised messenger of water deficit conditions is the phytohormone abscisic acid (ABA). Cellular ABA levels are detected by a class of soluble ABA receptors of the PYRABACTIN RESISTANCE/PYRABACTIN RESISTANT-LIKE/REGULATORY COMPONENT OF ABA RECEPTOR (PYR/PYL/RCAR) protein family (hereafter referred to as PYLs). ABA-bound PYLs interact with PROTEIN PHOSPHATASES 2C (PP2Cs) that act as negative regulators of ABA signalling (Ma et al., 2009; Miyazono et al., 2009; Park et al., 2009; Rubio et al., 2009; Santiago et al., 2009). The repressive role of PP2Cs is exerted through their binding to SUCROSE-NON-FERMENTATION KINASE SUBFAMILY 2 (SnRK2s) proteins, causing repression of their kinase activity (Umezawa et al., 2009; Vlad et al., 2009). Thus, ABA-stimulated PYLs inhibit PP2Cs so that the SnRK2s can initiate ABA responses. Activated SnRK2s quickly phosphorylate and activate multiple target proteins, including transcription factors (TFs) that control ABA-responsive genes (Fujii et al., 2009; Furihata et al., 2006; Minkoff et al., 2015; Umezawa et al., 2013; Wang et al., 2013). ABA-responsive element (ABRE)-BINDING FACTORS (ABFs), belonging to the basic leucine zipper (bZIP) family are master regulators of ABA-dependent transcriptional reprogramming (Fujita et al., 2011, 2005; Yoshida et al., 2015). However, integration of RNA-sequencing and Chromatin immunoprecipitation (ChIP)-seq studies revealed additional levels of complexity associated with ABA transcriptional responses, orchestrated by a wide network of TFs with different binding dynamics and combinatorial interactions at

target genes promoters (Song et al., 2016). Coordination of these transcriptional events may dictate the regulation of ABA production and sensitivity in space (tissue types) and at different timescales, appropriate with the different water stress conditions. While ABA is the major regulator of plant gas exchange, the molecular mechanisms that control the diel organization of its responses are only beginning to emerge (Dubois et al., 2017; Endo et al., 2008; Fukushima et al., 2009). One key mechanism relies on the circadian clock that affords coordination of physiological and metabolic processes according to transpiration demands. Stomatal opening, photosynthetic rates, carbon metabolism and assimilation impact lifetime biomass accumulation and also drought tolerance (Dodd et al., 2005; Nakamichi et al., 2016; Simon et al., 2020). Downstream of the core clock oscillator, several mechanisms may restrict specific transcriptional programs at specific times. *GIGANTEA* (*GI*), encoding a plant-specific gene, has been implicated in multiple signalling cascades, including the regulation of circadian rhythms and several plant environmental responses (Fowler et al., 1999; Huq et al., 2000; Martin-Tryon et al., 2007; Mizoguchi et al., 2005; Park et al., 1999). *GI* transcript and protein follow a similar diel accumulation pattern, with peaks occurring at approximately midday in a typical long day photocycle of 16h (Fowler et al., 1999; Park et al., 1999). This oscillatory pattern of GI is associated with the regulation of different sets of genes within the circadian cycle, thereby controlling numerous phenotypic traits (Mishra and Panigrahi, 2015). The activation of photoperiodic flowering is one of the best-studied modes of action of GI with respect to transcriptional regulation. GI binds to the blue light photoreceptor FLAVIN-BINDING, KELCH REPEAT, F-BOX 1 (FKF1) to promote degradation of CYCLING DOF FACTORs (CDFs) that repress the floral activator *CONSTANS* (*CO*) and *FLOWERING LOCUS* (*FT*) (Fornara et al., 2009; Imaizumi et al., 2005; Sawa et al., 2007). Interestingly, the GI-CDFs module regulates freezing tolerance in *Arabidopsis,* pointing to a wider contribution of this transcriptional mechanism to gene regulation (Fornara et al., 2015; Kim et al., 2012). GI has been described as a scaffold for direct interaction with the blue light photoreceptor (and FKF1 homologue) ZEITLUPE (ZTL). GI promotes ZTL accumulation and, in turn, ZTL proteolytic activity against TIMING OF CAB EXPRESSION 1 (TOC1), a transcription factor that controls clock function (Ito et

al., 2012; Kim et al., 2007). Thus, one clear mode of GI influence on transcriptional events is through FKF1 and ZTL, stimulating targeted protein degradation of their specific targets.

GI can be found in different protein complexes (Ito et al., 2012; Krahmer et al., 2019), including nuclear complexes that control its own stability and localization to regulate chromatin accessibility (Y. Kim et al., 2013; Yu et al., 2008). As GI protein lacks a recognized DNA binding domain, its association with DNA regulatory elements may be indirect, possibly mediated by a variety of TFs (Baek et al., 2020; Kubota et al., 2017; Nohales et al., 2019; Sawa and Kay, 2011). The association between GI and different TFs may explain the high level of phenotypic pleiotropy described in *gi* mutants, including enhanced resistance to oxidative stress (Kurepa et al., 1998) and salt stress (W. Y. Kim et al., 2013) which cannot be ascribed to the above well-characterised GI interactors. Despite the importance of GI in gene-environment regulation across plant species (Izawa et al., 2011), little is known about its role in regulating transcriptional responses elicited by water deficit. *gi* mutants present signatures of ABA deregulated gene expression in the absence of external stress suggesting a role in mediating water deficit signals (Fornara et al., 2015; Kim et al., 2012) and GI function is sensitive to ABA signalling (Riboni et al., 2016). Physiological data support a role for GI in promoting stomatal opening and thus water loss (Ando et al., 2013), and in activating ABA biosynthetic genes (Baek et al., 2020). In this work we describe GI as a key component of ABA-regulated transcriptional outputs. The observed patterns of gene expression and mutant analyses are consistent with a model where GI establishes diurnal oscillations in ABA sensitivity so that peak GI accumulation leads to a phase of minimal ABA sensitivity and maximal transpiration.

Results and discussion

GI represses ABA responses in a phase specific manner

We determined the contribution of *GI* in controlling ABA signalling and responses by analysing differentially expressed genes (DEGs) in *gi-2* mutant plants subject to water deficit. DEGs were also compared to strong ABA deficient mutant plants (*aba1-6*), and wild-type Columbia (Col-0) plants undergoing the same conditions.

Samples derived from plants grown for 3-week-old under short day photoperiods (SDs) and undergoing either water deficit or well-watered conditions before shifting to long days (LDs), while maintaining the same irrigation scheme (well-watered and water deficit, maintained by gravimetric measurements) (Figure 1A). This experimental design enabled us to synchronise plants at the vegetative stage and to control for potential effects on gene expression caused by the different developmental stages of the genotypes. It also allowed us to evaluate the impact of GI on ABA/water deficit -regulated traits before and after photo stimulation of the photoperiodic pathway (i.e., when the role of GI is best described) as we sampled tissues at different times in the day including ZT1, (Zeitgeber Time 1, i.e., within 1 hour after dawn of the last SD) and the remaining time points capturing the end of the last SD (ZT8) and the photo-extension to LD (ZT12 and ZT16) (Figure 1A).

In the wild type, water deficit resulted in a statistically significant deregulation of genes at all the time points considered. A slight over representation of repressed genes compared with normal irrigation was observed (Figure 1B). At every time point, pairwise comparisons of sets of DEGs revealed both common and time-of-the-day-specific patterns of expressions (Figure 1C). The observation that water deficit could impose strong and specific gene deregulations already in the morning timepoint (ZT1) may support a model of anticipation of expression of drought tolerance-related genes to prepare for higher transpiration demand later in the day (Mizuno and Yamashino, 2008). We recovered a total of 4780 distinct individual DEGs (FDR < 0.05) by comparing mutants to wild type plants, at any given time-point and irrigation condition (Table S1). Principal component analysis (PCA) of log normalised DEGs expression levels revealed that the most extreme difference in gene expression (PC1, 39%) was observed between time of the day ZT1 and the remaining time points (ZT8, ZT12 and ZT16) across all genotypes (Figure 1D). PC2 broadly reflected the contribution of genotype and treatment but explained smaller proportions of the variation in gene expression (19% of the variability of the DEGs). Interestingly, the *gi* mutant displayed less separation compared with ABA deficient mutants and the wild type on both the first (time points) and second (genotype/treatment) components of the PCA, suggesting a deregulation in the diel

responses to water deficit stimuli in *gi* mutant plants compared to the other genetic backgrounds analysed in this study.

We could detect a remarkable separation of gene expression patterns between morning DEGs detected at ZT1 and the remaining time points. Based on the consideration that ZT8, ZT12 and ZT16 clustered together in our PCA, and that ZT12 could coincide with light-dependent stimulation of the photoperiodic cascade (Sawa et al., 2007), we selected the ZT1 and ZT12 time points to perform more detailed analyses. GI function had a large impact on gene expression at ZT12 compared with ZT1, with a clear prevalence of upregulated genes at ZT12 under well-watered and water deficit conditions when the number of DEGs increased up to 2.4-fold compared to control conditions (1817 vs 730 DEGs, respectively) (Figure 2A,B). A similar over representation of upregulated genes in *gi* mutants occurred at ZT8 and ZT16 compared with the wild type and similar observations were made in direct comparisons with *aba1* mutants (Figure S1), further supporting a general repressive role of GI on water deficit-regulated gene expression.

The analysis of *GI* transcript accumulation across different ZTs revealed a peak in accumulation at ZT8 with negligible variations observed in response to water deficit or ABA deficiency (Figure S2). Based on prior reports (Sawa et al., 2007), GI protein accumulation broadly reflects its transcript levels, indicating that the large increase in DEGs detected at ZT12 does not coincide with the peak of GI accumulation. This could point to additional molecular mechanisms mediated by GI that are dependent on the extended light period, namely the light-dependent interaction with blue light photoreceptors. Despite this observation, a large proportion of DEGs in *gi* mutants were common between ZT1 and ZT12 (Figure 2C) and intersections of sets of DEGs were statistically significant between any time point (hypergeometric distribution p-values all <= 1E-33). Moreover, a sizable fraction of GI-DEGs at ZT1 and ZT12 (39% and 66%, respectively) observed under normal irrigation conditions were also deregulated under water deficit at matched time points. Thus, even in the absence of water deficit stress *gi* plants already present alterations in the water deficit-regulated transcriptome. As water deficit caused an increased representation of upregulated genes in *gi*, we tested the possibility that this could depend on an interaction between the genotype and water deficit (i.e., an

amplification of water deficit-mediated gene upregulation in the absence of GI function). We compared fold change of expression of GI-DEGs under water deficit at ZT12 (*gi* vs. wild type) to changes in gene expression observed under water deficit vs. control in the wild type and *gi* mutants, respectively (Figure 2D). Strikingly, water deficit caused a global downregulation of these genes in the wild type, and no consistent upregulation could be observed in *gi* plants under water deficit compared with control conditions. These observations suggest that GI contributes to repress expression of these genes and water deficit inputs have a limited contribution in driving further gene upregulation in *gi* mutants. Genes that were upregulated in the wild type in response to water deficit had similar levels of expression in *gi*, independent of water deficit conditions. However, these genes displayed a higher level of variability in their expression patterns compared with genes that were downregulated in the same condition (coefficient of variation of the logFC distribution = 55.3 and 3.4, respectively for the up- and down- regulated genes), suggesting that GI-activated genes are more significantly influenced by water deficit conditions in the absence of GI.

In the ABA deficient mutant background *aba1* a higher number of DEGs was recovered at ZT1 compared with ZT12 (Figure S3). Water deficit conditions strongly amplified this time-of-the-day dependency on ABA-DEGs (547 DEGs under normal irrigation vs 1610 under water deficit), when we observed a mild over-representation of down regulated genes. These patterns of gene deregulation may reflect diel oscillations of ABA production, which peaks at dusk (Adams et al., 2018; Fukushima et al., 2009). In this view and since severe ABA deficient mutants like *aba1-6* can synthesize small quantities of ABA (Rock and Zeevaart, 1991), *aba1-6* plants may have the lowest point of ABA accumulation in the morning with a gradual recovery at later time points (Figure S3). Despite the different diel contribution of GI signalling to gene regulation under water deficit conditions we could detect highly significant overlaps between ABA and GI DEGs both at ZT1 and ZT12 time points, under both well-watered conditions (53 and 66 common DEGs at ZT1 and ZT12, respectively) or water deficit (419 and 400 common DEGs, at ZT1 and ZT12, respectively) (Figure S3). Our data suggest that diel changes in GI accumulation

cause different phases of ABA sensitivity whereby high levels of GI signalling at ZT12 contribute to repress ABA responses.

GI binding overlaps with different classes of TFs and is associated with the repression of target genes

The increased number of shared DEGs in *aba1* and *gi* plants under water deficit points to a convergence of GI and ABA signalling to gene regulation. Cis motif analysis at the promoter regions (1000 bps upstream of the transcription start site - TSS) of ABA and GI DEGs predicted significant enrichments for several TFs binding sites. We computed scores for binding sites enrichment at DEGs detected under different combinations of genotype comparison/treatment/time point (Table S2). Focusing on the binding motifs detected in DEGs common among ABA and GI DEGs under water deficit, we found an over-representation for bZIPs transcription factors binding (including ABA INSENSITIVE 5, p value = 2.23E-25 at ZT1 and related ABF2, p value = 1.76E-22 at ZT1) which are key in coordinating ABA-dependent transcriptional responses and PHYTOCHROME-INTERACTING FACTORs (PIFs) (PIF4, p value = 6.84E-18 at ZT1), acting as central components of plant photomorphogenesis (Leivar and Monte, 2014) (Figure 3A). While there are no obvious indications about the role of PIFs in response to drought stress in *Arabidopsis*, recent data indicate that their binding at target chromatin regions is negatively regulated by GI (Nohales et al., 2019). We also detected a significant enrichment of CDF binding sites (CDF2, p value = 2.80E-03 at ZT1) at the promoter of ABA and GI DEGs, consistent with their role in conferring plant survival upon freezing temperature (Fornara et al., 2015) and drought (Corrales et al., 2017).

A meta-analysis of a selection of ChIP-seq datasets of known ABA-related transcription factors (Song et al., 2016) and PIF proteins (Pfeiffer et al., 2014) confirmed the strong enrichment for the binding of ABFs and PIFs at the promoters of ABA and GI DEGs (Table S3). PIFs and ABFs direct targets were more represented under water deficit conditions, irrespective of the time point, and were not associated with a clear direction of regulation (Figure 3B). Most DEGs in *gi* or *aba1* mutants were also targets of both ABFs and PIFs, suggesting cooperation

between these families of TFs at target genes promoters and pointing to contribution of PIFs in coordinating drought stress responses.

Many other ABA-regulated families of TFs were similarly and significantly enriched in the promoters of our lists of DEGs, potentially indicating a pervasive role of GI in the regulation of ABA transcriptional responses (Table S3). GI ChIP-seq peaks were found to be significantly associated with the promoters of both *gi* and *aba1* mutants DEGs (Table S3). GI binding was also significantly more associated with upregulation of the target genes detected in *gi* mutants (Fisher's exact test p value = 1.09E-02), confirming the predominantly repressive role of GI with respect to gene expression (Figure 3C). The comparison of independent ChIP datasets allowed us to uncover a general and significant overlap between ABA-regulated TFs and GI binding peaks (Table S4). As these comparisons included different families of transcriptional regulators, these results could point to a direct role for GI at the regulatory chromatin of ABA-responsive genes, in cooperation or competition with different TF families. Such a general association between GI and several families of TFs offers intriguing insights into the complexity of the molecular interplay between different TFs and their target genes upon water deficit conditions. In this scenario GI might alter the stability, activation, or occupancy potential of TFs in a phase specific manner.

GI regulates ABA signalling genes but not ABA accumulation

Similarities in gene deregulation patterns between *gi* and *aba1* do not derive from altered ABA accumulation in *gi* mutants. Unlike recent reports, we found no significant deregulation in the levels of the rate limiting ABA metabolic genes *9-CIS-EPOXYCAROTENOID DIOXYGENASE 3* (*NCED3*) under well-watered conditions (Baek et al., 2020) nor other ABA metabolic or catabolic genes in *gi* mutants (Figure S2, Table S1). A slight, but significant, decrease in *NCED3* transcript accumulation was observed under water deficit conditions in *gi* mutants at ZT12 and ZT1 (Figure 4A, Figure S2 and S4). To further verify the possible role of GI in promoting ABA accumulation under water deficit conditions, we conducted an independent experiment to measure total ABA accumulation. Samples derived from plants grown under water deficit conditions or well-watered conditions in a

continuous LD photoperiod. We harvested tissue at ZT10, which coincides with high GI-stimulated photoperiodic signal stimulation (Sawa et al., 2007). To control for the different developmental stages of *gi* and wild-type plants under LDs we also analysed *co* and *fkf1* mutants, which are phenotypically comparable to *gi* with respect to the duration of the vegetative phase and growth but are defective at different steps of the photoperiodic cascade. Basal levels of ABA accumulation under normal irrigation conditions were similar in all the genotypes considered (Figure S5). Cellular ABA accumulation increased in wild-type plants undergoing water deficit, but similarly so in *gi*, *fkf1* and *co* mutants. Thus, our data are more consistent with a model where GI regulates ABA-responses or signalling via modulation of transcriptional processes.

Gene Ontology analysis revealed both common and unique functions associated with GI-DEGs at ZT1 and 12 under normal irrigation conditions (Figure S6). DEGs at ZT1 and ZT12 were particularly enriched in carbohydrate metabolic processes and photosynthesis-related functions respectively, which could be linked to the known role of GI in carbon metabolism and sugar hold-release signalling (Dalchau et al., 2011; Eimert et al., 1995; Mugford et al., 2014). Notably, DEGs related to "response to abiotic stimulus" and "water deprivation" were significantly enriched under control conditions at ZT12 and ZT1, respectively. As expected, most gene responses observed under water deficit conditions were associated with water deprivation terms, irrespective of the time point analysed.

Despite the known interplay between the circadian clock and ABA-related responses (Mizuno and Yamashino, 2008; Seung et al., 2012), we found limited examples of deregulation of core circadian clock genes in response to the water deficit conditions used in this study, which extends similar observations under mild drought scenarios (Dubois et al., 2017). A notable exception to this pattern was *TOC1* which was similarly and significantly upregulated in *gi* and *aba1* plants under water deficit at ZT1 (Figure S4). Such an increase in *TOC1* transcript levels may translate into elevated TOC1 protein abundance in *gi* mutant plants, as GI mediates the proteolytic degradation of TOC1 in association with blue light stimulated F-box protein ZTL at dawn (Kim et al., 2007). Furthermore, *TOC1* over-expression causes reduced ABA sensitivity of guard cells, constitutive stomata opening and decreased plant survival

under drought conditions (Legnaioli et al., 2009). By comparing changes in DEGs previously assigned to circadian clock regulation (Covington et al., 2008), we confirmed an over-representation for circadian clock-controlled genes among the *GI* DEGs at time points representative of morning and dusk, particularly under water deficit (Figure S7). A similar high representation for circadian genes was observed for ABA DEGs, confirming the enrichment for ABA-regulated processes among circadian-related genes (Covington et al., 2008).

Previous studies also defined a set of ABA-responsive genes under circadian controls including *EARLY RESPONSE TO DEHYDRATION* (*ERD*) *7*, *COLD-REGULATED* (*COR*) *15A* and *B* (Mizuno and Yamashino, 2008). Besides verifying that the accumulation of these genes was ABA-dependent we also found a general and significant pattern of increased accumulation in *gi* mutants compared with the wild type (Figure 4A,B, Figure S2 and S4). This pattern of deregulation was previously associated with the increased freezing tolerance of *gi* mutant plants (Fornara et al., 2015; Kim et al., 2012).

We set up an independent experiment to test if overexpression of *GI* could reduce the accumulation of these ABA-regulated markers. We compared *35S::HA-GI* plants with the wild type, upon exogenous ABA applications or in control conditions after two weeks of growth on soil under a long day photocycle and measured transcript levels by quantitative real time PCR. Under control conditions, *COR15A* and *ERD7* transcripts accumulation followed a strong daytime-dependent increase in the wild type, with higher levels of accumulation detected at ZT8 compared to ZT1. At ZT8, we observed a significant decrease in these transcripts levels in *35S::HA-GI* plants compared with the wild type (factorial ANOVA analysis p = 7.90E-03 and 4.97E-02 for *COR15A* and *ERD7*, respectively) (Figure S8). Upregulation of *COR15A* in response to ABA (i.e., the slope) was significantly stronger in *35S::HA-GI* plants, while overall ABA-dependent accumulation of these markers in *35S::HA-GI* plants reached similar levels of the wild type. Thus, under physiological, non-stressed conditions *GI* can reduce the accumulation of these genes, but an acute increase in cellular ABA concentration (as in this condition) may ultimately overcome GI-repressive function despite the 5-6 fold excess of *GI* accumulation detected at ZT8 in *35S::HA-GI* plants compared with the wild type (Figure S8).

RNAseq analysis of other ABA responsive target genes including *MITOGEN-ACTIVATED PROTEIN KINASE KINASE KINASE 18* (*MAPKKK18*), *Rab-related gene 18* (Lång and Palva, 1992; Mitula et al., 2015) did not reveal significant variations between the genotypes analysed under water deficit conditions (Figure 4A,B Figure S2 and S4). This could be due to transcriptional desensitization of ABA downstream targets upon prolonged water deficit conditions (Asensi-Fabado et al., 2017). The ABA-regulated *MYB96* transcription factor (Lee et al., 2016), controlling ABA sensitivity in the evening was slightly (but not significantly) upregulated in *gi* mutants, which could contribute to increase ABA responses. However, no further upregulation was observed under water deficit condition (Figure S2).

Inspection of genes associated with ABA signalling in *gi* plants at ZT12 revealed a general and significant downregulation of clade A *PP2C*-encoding genes *ABI1*, *ABI2* and *HIGHLY ABA-INDUCED* (*HAI*) *1* and *2*, the proteostasis – related *ABI FIVE BINDING PROTEIN* (*AFP*) *1* and *3* genes, which function as negative regulators of ABA signalling (Bhaskara et al., 2012; Leung et al., 1997; Lopez-Molina, 2003) and a slight upregulation of the ABA receptor *PYL4* (Figure 4A). The reduced levels of *PP2Cs ABI1*, *ABI2* transcript levels in *gi* plants undergoing water deficit was further verified by quantitative real-time PCR analysis on the same time points analysed by RNAseq and across additional time points encompassing the previous short day and the subsequent long day (Figure S9). This pattern of accumulation of ABA signalling and responsive genes echoed that observed in *aba1* mutants (Figure 4B and Figure S9) which would be expected as results of impaired ABA transcriptional responses (Wang et al., 2019). Because we found downregulation of clade A *PP2Cs* and upregulation of *PYL4*, our data support a role for GI in regulating the early steps of the ABA signalling cascade, which could further impact ABA-regulated gene expression. Previously we detected an over representation for ABA-regulated bZIPs at the *GI*-regulated promoters under water deficit (Figure 3B). Transcript levels of *ABF3* and *ABF4* did not change in *gi* mutants compared with the wild type at ZT12, pointing to post-transcriptional effects (Figure 4A). As loss in *PP2Cs* function results in increased ABA responsiveness (Bhaskara et al., 2012; Rubio et al., 2009), GI may normally act to repress ABA signalling at this time of the day at multiple levels, by

de-sensitising the core ABA signalling cascade, and by interfering with TFs (e.g., the ABFs) function.

GI regulates phase specific ABA sensitivity to control transpiration

We next examined the role of GI in regulating ABA-specific physiological traits. We measured leaf surface temperatures, which is highly related to transpiration through stomata (Yang et al., 2016). Stomatal movement is regulated via ABA through rapid post-transcriptional activation of ion channels localised at the plasma membrane (Munemasa et al., 2015). Thus, changes in ABA signalling and response in *gi* guard cells should cause alterations in water loss compared with the wild type, which can be monitored using an infrared imaging approach. To control for the different development of wild-type and *gi* plants we analysed plants undergoing a shift from short to long days, with data collected on the second long day (Figure 5A). We evaluated the impact of *gi* on leaf temperature in response to ABA treatment at three time periods (ZT1, ZT8, and ZT16) using a factorial linear model. We tested for the main effect of genotype (*gi* vs. wild type), treatment (mock vs. ABA applications), or their interaction across each time period. Here, a significant interaction indicates that the effect of *gi* mutation on leaf temperature differed from wild type in response to ABA treatment. At ZT1 and ZT16 we discovered simple main effects of Genotype and Treatment. At both of these ZTs, ABA treatment slightly increased leaf temperature (T; $P<0.05$). At ZT1, the wild type had higher leaf temperature compared to *gi* and the reverse was true at ZT16 (G; in both cases $P<0.05$). However, genotype responses to ABA were similar (GxT $p>0.05$) at these time points. In contrast, we detected a significant Genotype x Treatment interaction at ZT8. Here, the *gi* mutant showed a stronger increase in leaf temperature in response to ABA treatment compared to the wt (GxT; $P=0.008$) (Figure 5B). The detected patterns of warmer leaf temperature observed in *gi* mutants at ZT8 and ZT16 may reflect the consequences of time-of-the day changes in GI function as a repressor of ABA-regulated processes. Notably, impairing GI function caused increased sensitivity to ABA compared with the wild type, but only at ZT8. This indicates that other layers of ABA responsiveness are regulated independent of GI function.

In summary, our study provides a framework for defining how GI exerts multilevel influence on ABA-regulated gene expression, ABA signalling sensitivity, and the phenotypic traits that depend on these molecular processes. Our data indicate that GI acts as a general hub for the ABA transcriptional network, in conjunction with multiple TFs families. GI was recently shown to prevent PIFs binding to chromatin via direct interaction (followed by PIFs degradation) and competition at chromatin region (Nohales et al., 2019). Here we extend this model to suggest that GI may exert similar regulatory roles on many other TFs to gate ABA responses according to diurnal cycles of GI accumulations (Figure 5C).

Materials and Methods

Plant material and growth conditions

In this study we used wild–type *Arabidopsis* plants, ecotype Columbia (Col–0), transgenic lines *35S::HA-GI* (David et al., 2006) and mutant lines *aba1-6* (Niyogi et al., 1998), *gi-2* (Fowler et al., 1999), *gi-100* (Huq et al., 2000), *fkf1* line SALK_059480 (Riboni et al., 2013), *co-10* (Laubinger et al., 2006). Seeds were germinated and plants grown in a controlled environment at a temperature of 21-23 °C, 65% relative humidity, either under long day (16 h light / 8 h dark) or short day (8 h light / 16 h dark) photocycles. Light was cool white fluorescent tubes (Osram, Sylvania) at a fluency of 120–150 $\mu mol\ m^{-2}\ s^{-1}$ (Photosynthetically active radiation). Water deficit conditions were imposed two days after germination, so that under normal irrigation conditions plants grew under a Relative Soil Water Content (RSWC) of 80 – 90%, and 30% RSWC under water deficit (Riboni et al., 2013). RSWC was kept constant throughout the experiment (i.e., during the short day and long day part) by daily weighing of pots and applications of water to maintain the desired values. Samples used for RNA-seq analysis (or real time PCR) derived from

an experiment previously described (Riboni et al., 2013). For each time point / treatment / genotype combination, we analysed two biological replicates, each one consisting of approximately 50 seedlings pooled from three different Arabasket pots.
ABA quantification derived from an independent experiment. Stratified seeds (20–50) were sown in Arabasket pots and grown under water deficit irrigation (or control) for 20 days in a growth chamber set under long day photocycle. Plants were harvested at ZT10 in three biological replicates, and each replicate consisting of 100 mg of pooled seedlings derived from 2-3 independent Arabasket pots. To avoid soil carryover, we harvested only the aerial part of plants (i.e., above the hypocotyl).
To quantify gene expression in response to exogenous ABA, plants were grown in Arabasket pots (at a density of approx. 20 seedlings in each pot) under normal irrigations for two weeks (after germination) in a long-day growth chamber (as above). On the evening of the 15th day plants were sprayed with 10 μm ABA or a mock solution. Sampling occurred on the following day at ZT1 and ZT8 and four replicates for each genotype/timepoint/treatment combination were harvested from independent pots.

RNAseq and expression analysis by real time PCR

RNA was extracted using the Trizol reagent (Invitrogen). For RNA sequencing, RNA Quality Control was performed with an electrophoretic run on a Bioanalyzer instrument using the RNA 6000 Nano Kit (Agilent). RNA Integrity Number was determined, and all the samples were considered suitable for processing (RIN > 8). RNA concentration was estimated through a spectrophotometric measurement using a Nanoquant Infinite M200 instrument (Tecan). Sequencing libraries were prepared using the TruSeq™ RNA Sample Preparation Kit (Illumina). Polyadenylated transcripts were purified using poly-T oligo-attached magnetic beads. PolyA RNA was fragmented at 94 °C for 8 min and retrotranscribed using random hexamers. Multiple indexing adapters were ligated to the ends of the cDNA and the amount of DNA in the library was amplified by PCR. Final libraries were validated and quantified with the DNA1000 kit on the Agilent Bioanalyzer Instrument. Pooled libraries were sequenced on the Illumina Genome Analyzer IIx producing 72nt paired-end reads.

Reads were mapped on the reference assembly of *Arabidopsis thaliana* genome TAIR vs.10 as available from ftp://ftp.arabidopsis.org/home/tair) using the bowtie2 program (Langmead and Salzberg, 2012). Estimation of gene expression levels was performed using RSEM (Li and Dewey, 2011) and the TAIR10 annotation of gene models. Summary statistics concerning total number of reads, total number of mapped reads and number of unambiguously mapped reads are reported in Supplementary Table S5. Identification of differentially expressed genes was performed by the quasi-likelihood F-test as implemented by edgeR (Robinson et al., 2009). A False Discovery Rate (FDR) cut-off value of 0.05 was applied for the identification of significantly differentially expressed genes. Functional enrichment analysis of sets of differentially expressed genes were performed by means of ShinyGO, terms from the "biological process" domain of the Gene Ontology (GO) were set as the "pathway database" (Ge et al., 2020). Only the top 10 terms with most statistically significant enrichment were included in the graphical representation of the results enclosed in Supplementary Figure S6. Quantitative real-time PCR, changes in gene expression were calculated relative to *ACTIN2*. Values were either expressed as fold change variations relative to the wild type (ΔΔCt) or expressed as -ΔCt values (Castelletti et al., 2020) and analysed by fitting a factorial ANOVA model (ZT, genotype, treatment, genotype x treatment). Quantitative real-time PCR primers are provided in Supplemental Table S6.

ABA quantification

ABA was quantified according to the method described by (Salem et al., 2020) with minor modifications. Briefly, ABA was extracted from freeze-dried leaves (10 mg) after grinding to a powder using 1 mL of pre-cooled (-20°C) extraction solvent (methyl-tert-butyl-ether:methanol, MTBE:MeOH, 3:1, v:v). The extracted samples were vortexed and incubated on an orbital shaker at 4 °C for 30 min. Liquid-liquid phase separation was induced by adding a volume of 0.5 ml of acidified water (0.1% HCl) followed by 30 min incubation on an orbital shaker at 4 °C. The samples were centrifuged at 4 °C for 5 min at 13.000 x g and 1 mL from the MTBE layer was then evaporated in a vacuum concentrator before re-dissolving the residue in 100 µL of methanol: water (1:1, v/v). ABA was analysed by ultra-performance liquid

chromatography coupled to mass spectrometry (UPLC-MS/MS) analysis. The LC-MS analysis was performed on a quadruple linear ion trap mass spectrometer (4000 QTRAP MS/MS System, SCIEX, Redwood City, U.S.A.) connected to an Acquity ultra performance liquid chromatography (UPLC, Waters, Milford, MA, USA). The UPLC was equipped with a reversed-phase HSS T3 C18 column (100 mm×2.1 mm× 1.7 µm particles, Waters). ABA was identified and quantified using a multiple reaction monitoring (MRM) method (Salem et al., 2020).

Thermal Imaging

For leaf temperature analysis, plants were grown in 2-inch pots randomized in 32 cell trays. Trays were also randomly cycled between the top and bottom shelves in a short-day growth chamber (8 h light period, 22°C, a light intensity of 90 to 110-µmol m^{-2} s^{-1}). Pots were bottom watered with hyponex nutrient solution (~1 g L21) as needed. On the 8th day, seedlings were thinned to leave one plant per pot. On the 29th day (when plants were ~4-week-old), replicates were split into treatment and sprayed with 10 µm ABA or a mock solution. These were shifted to long days (16 h light). The following day, thermal imaging (FLIRA325sc) was carried out on whole plant trays at three time points (ZT1, ZT8, and ZT16). Leaf temperature was measured using FLIR ResearchIR Max4 software. We used the freehand ROI (Region of Interest) tool to trace the entire rosette carefully to avoid background and obtained the mean temperatures for individual rosettes.

Transcription factor binding analyses

The pscan software (Zambelli et al., 2009), in conjunction with the JASPAR_fam matrices set (Vlieghe et al., 2006), was used to calculate transcription factor binding site (TFBS) family score enrichment profiles for promoters (1000 bp upstream of TSS).

Publicly available ChIP-seq peaks for a selection of Transcription Factors were obtained from the GEO repository, under the following accessions GSE129865 (GI), GSE35059 (PIF5), GSE35315 (PIF4 etiolated seedling), GSE39215 (PIF3), GSE43283 (PIF1), GSE43284 (PIF 4 seedling 3 days), GSE68193 (PIF4 and PIF 5, seedling, 5 days), GSE80564 (Song et al., 2016). Genomic coordinates of promoter

sequences, defined as -1000 bp upstream and +100 bp downstream of an annotated TSS, based on the TAIR10 annotation of the reference *A. thaliana* genome were obtained by a custom Perl script.

Intersection of promoters and ChIP-seq peaks coordinates were performed by means of the bedtools intersect utility. Total number of overlaps were recorded by the means of a custom Perl script. A statistical test based on the hypergeometric distribution was applied to infer statistical significance. The total number peaks was used as the "total number of successes" in the population (k), while the size of the population was set to the total number of promoters in the genome as defined by the criteria outlined above. P-values were corrected by applying the Benjamini-Hochberg procedure for the control of False Discovery Rate.

Graphical representation and statistical analyses

Graphical representations of the data and comparisons between the raw data and published data sets were prepared with R software (R Core Team, 2020, https://www.R-project.org/). The Base R was used in combination with packages ggplot2 3.3.3 (Wickham, 2016), pheatmap 1.0.12, rstatix 0.6.0. For the PCA calculation the R base method using the singular value decomposition was applied (prcomp, R base). The input for PCA was a matrix of log2 scaled transcript abundance values for each gene in different conditions. For the final PCA displays the values referring to genes occurring as significantly altered in any given comparison were used. Heatmaps for motif analysis were generated with the pheatmap package (Raivo, 2012). Leaf temperature data were analysed by three-way repeated measures ANOVA with rstatix R package (Kassambara, 2021) considering genotype (*gi* mutant vs. wild type), treatment (ABA addition versus mock) and their interaction as fixed factors at each time point (ZT1, ZT8, ZT1) separately. The outliers in the data were identified based boxplot method and eliminated from analysis. Values above Q3+1.5xIQR (Inter Quantile Range) or below Q1-1.5xIQR were considered as outliers. Q1 and Q3 are the first and third quartile, respectively. IQR is the interquartile range (IQR = Q3 - Q1). The data was tested for normal distribution by Shapiro-Wilk's test of normality and the homogeneity of variance was assessed by Leven's test of homogeneity of variance. The significant two-way

interactions were further analysed as simple main effects to investigate the effect of genotype on leaf temperatures at each level of treatment. The R script used for the leaf temperature data analysis and visualization can be found here https://github.com/BhaskaraGB/ABA_photoperiod_GI.

Data availability

The data discussed in this publication have been deposited in NCBI's Gene Expression Omnibus (Edgar et al., 2002) and are accessible through GEO Series accession number GSE181083 (https://www.ncbi.nlm.nih.gov/geo/query/acc.cgi?acc=GSE181083).

Funding

'This work was supported by the Human Frontier Science Program [RGP0011/2019 - An integrative approach to decipher flowering time dynamics under drought stress] - to LC and TJ, and the University of Milan, [SEED 2019, DISENGAGE] to LC.

Acknowledgments

We would like to acknowledge George Coupland and the Nottingham Arabidopsis Stock Centre (NASC) for providing seeds lines. We also thank Fabio Fornara, Vittoria Brambilla (University of Milan) Takeshi Izawa (University of Tokyo) and Xiaoyu Weng (UT at Austin) for insightful comments on the manuscript. We thank personnel at Orto Botanico Città Studi for plant care.

Author contributions

BS, MC, BGB, MR, FD, DB, MAAS, investigation with help from DM and SC who contributed with supervision and data curation. CT, MG, PG, TEJ and LC conceptualisation and methodology. BS, MC, BGB Visualisation and formal analysis. BS, MC and LC Writing – original draft. CT, MG, PG, TEJ and LC Writing – review & editing.

Conflicts of interest

No conflicts of interest declared

References

Adams, S., Grundy, J., Veflingstad, S.R., Dyer, N.P., Hannah, M.A., Ott, S., et al. (2018) Circadian control of abscisic acid biosynthesis and signalling pathways revealed by genome-wide analysis of LHY binding targets. *New Phytologist*. 220: 893–907.

Ando, E., Ohnishi, M., Wang, Y., Matsushita, T., Watanabe, A., Hayashi, Y., et al. (2013) TWIN SISTER OF FT, GIGANTEA, and CONSTANS have a positive but indirect effect on blue light-induced Stomatal opening in Arabidopsis. *Plant Physiology*. 162: 1529–1538.

Asensi-Fabado, M.A., Amtmann, A., and Perrella, G. (2017) Plant responses to abiotic stress: The chromatin context of transcriptional regulation. *Biochimica et Biophysica Acta - Gene Regulatory Mechanisms*. 1860: 106–122.

Baek, D., Kim, W.Y., Cha, J.Y., Park, H.J., Shin, G., Park, J., et al. (2020) The GIGANTEA-ENHANCED em LEVEL Complex Enhances Drought Tolerance via Regulation of Abscisic Acid Synthesis1[OPEN]. *Plant Physiology*. 184: 443–458.

Bhaskara, G.B., Nguyen, T.T., and Verslues, P.E. (2012) Unique drought resistance functions of the highly ABA-induced clade a protein phosphatase 2Cs. *Plant Physiology*. 160: 379–395.

Castelletti, S., Coupel-Ledru, A., Granato, I., Palaffre, C., Cabrera-Bosquet, L., Tonelli, C., et al. (2020) Maize adaptation across temperate climates was obtained via expression of two florigen genes. *PLOS Genetics*. 16: e1008882.

Corrales, A.R., Carrillo, L., Lasierra, P., Nebauer, S.G., Dominguez-Figueroa, J., Renau-Morata, B., et al. (2017) Multifaceted role of cycling DOF factor 3 (CDF3) in the regulation of flowering time and abiotic stress responses in Arabidopsis. *Plant Cell and Environment*. 40: 748–764.

Covington, M.F., Maloof, J.N., Straume, M., Kay, S.A., and Harmer, S.L. (2008) Global transcriptome analysis reveals circadian regulation of key pathways in plant growth and development. *Genome Biology*. 9: R130.

Dalchau, N., Baek, S.J., Briggs, H.M., Robertson, F.C., Dodd, A.N., Gardner, M.J., et al. (2011) The circadian oscillator gene GIGANTEA mediates a long-term response of the Arabidopsis thaliana circadian clock to sucrose. *Proceedings of the National Academy of Sciences*. 108: 5104–5109.

David, K.M., Armbruster, U., Tama, N., and Putterill, J. (2006) Arabidopsis GIGANTEA protein is post-transcriptionally regulated by light and dark. *FEBS Lett*. 580: 1193–1197.

Dodd, A.N., Salathia, N., Hall, A., Kévei, E., Tóth, R., Nagy, F., et al. (2005) Cell biology: Plant circadian clocks increase photosynthesis, growth, survival, and competitive advantage. *Science (1979)*. 309: 630–633.

Dubois, M., Claeys, H., Van den Broeck, L., and Inzé, D. (2017) Time of day determines Arabidopsis transcriptome and growth dynamics under mild drought. *Plant, Cell & Environment*. 40.

Edgar, R., Domrachev, M., and Lash, A.E. (2002) Gene Expression Omnibus: NCBI gene expression and hybridization array data repository. *Nucleic Acids Research*. 30: 207–210.

Eimert, K., Wang Shue-Mei, Lue Wei-Ling, and Chen Jychian (1995) Monogenic recessive mutations causing both late floral initiation and excess starch accumulation in Arabidopsis. *Plant Cell*. 7: 1703–1712.

Endo, A., Sawada, Y., Takahashi, H., Okamoto, M., Ikegami, K., Koiwai, H., et al. (2008) Drought induction of Arabidopsis 9-cis-epoxycarotenoid dioxygenase occurs in vascular parenchyma cells. *Plant Physiology*. 147: 1984–1993.

Fornara, F., De Montaigu, A., Sánchez-Villarreal, A., Takahashi, Y., Ver Loren Van Themaat, E., Huettel, B., et al. (2015) The GI-CDF module of Arabidopsis affects freezing tolerance and growth as well as flowering. *Plant Journal*. 81: 695–706.

Fornara, F., Panigrahi, K.C.S., Gissot, L., Sauerbrunn, N., Rühl, M., Jarillo, J.A., et al. (2009) Arabidopsis DOF Transcription Factors Act Redundantly to Reduce CONSTANS Expression and Are Essential for a Photoperiodic Flowering Response. *Developmental Cell*. 17: 75–86.

Fowler, S., Lee, K., Onouchi, H., Samach, A., Richardson, K., Morris, B., et al. (1999) GIGANTEA: A circadian clock-controlled gene that regulates photoperiodic flowering in Arabidopsis and encodes a protein with several possible membrane-spanning domains. *EMBO Journal*. 18: 4679–4688.

Fujii, H., Chinnusamy, V., Rodrigues, A., Rubio, S., Antoni, R., Park, S.Y., et al. (2009) In vitro reconstitution of an abscisic acid signalling pathway. *Nature*. 462: 660–664.

Fujita, Y., Fujita, M., Satoh, R., Maruyama, K., Parvez, M.M., Seki, M., et al. (2005) AREB1 is a transcription activator of novel ABRE-dependent ABA signaling that enhances drought stress tolerance in Arabidopsis. *THE PLANT CELL*. 17: 3470–3488.

Fujita, Y., Fujita, M., Shinozaki, K., and Yamaguchi-Shinozaki, K. (2011) ABA-mediated transcriptional regulation in response to osmotic stress in plants. *Journal of Plant Research*. 124: 509–525.

Fukushima, A., Kusano, M., Nakamichi, N., Kobayashi, M., Hayashi, N., Sakakibara, H., et al. (2009) Impact of clock-associated Arabidopsis pseudoresponse regulators in metabolic coordination. *Proc Natl Acad Sci U S A*. 106: 7251–7256.

Furihata, T., Maruyama, K., Fujita, Y., Umezawa, T., Yoshida, R., Shinozaki, K., et al. (2006) Abscisic acid-dependent multisite phosphorylation regulates the activity of a transcription activator AREB1. *Proc Natl Acad Sci U S A*. 103: 1988–1993.

Ge, S.X., Jung, D., and Yao, R. (2020) ShinyGO: a graphical gene-set enrichment tool for animals and plants. *Bioinformatics*. 36: 2628–2629.

Huq, E., Tepperman, J.M., and Quail, P.H. (2000) GIGANTEA is a nuclear protein involved in phytochrome signaling in Arabidopsis. *Proc Natl Acad Sci U S A*. 97: 9789–9794.

Imaizumi, T., Schultz, T.F., Harmon, F.G., Ho, L.A., and Kay, S.A. (2005) Plant science: FKF1 F-box protein mediates cyclic degradation of a repressor of CONSTANS in Arabidopsis. *Science (1979)*. 309: 293–297.

Ito, S., Song, Y.H., and Imaizumi, T. (2012) LOV Domain-Containing F-Box Proteins: Light-Dependent Protein Degradation Modules in Arabidopsis. *Molecular Plant*. 5.

Izawa, T., Mihara, M., Suzuki, Y., Gupta, M., Itoh, H., Nagano, A.J., et al. (2011) OsGIGANTEA Confers Robust Diurnal Rhythms on the Global Transcriptome of Rice in the Field. *The Plant Cell*. 23: 1741.

Kassambara, A. (2021) rstatix: Pipe-Friendly Framework for Basic Statistical Tests. R package version 0.7.0. .

Kim, W.Y., Ali, Z., Park, H.J., Park, S.J., Cha, J.Y., Perez-Hormaeche, J., et al. (2013) Erratum: Release of SOS2 kinase from sequestration with GIGANTEA determines salt tolerance in Arabidopsis (Nature Communications (2013) 4 (1352) DOI:10.1038/ncomms2357). *Nature Communications*. 4: 1820.

Kim, W.Y., Fujiwara, S., Suh, S.S., Kim, J., Kim, Y., Han, L., et al. (2007) ZEITLUPE is a circadian photoreceptor stabilized by GIGANTEA in blue light. *Nature*. 449: 356–360.

Kim, Y., Lim, J., Yeom, M., Kim, H., Kim, J., Wang, L., et al. (2013) ELF4 Regulates GIGANTEA Chromatin Access through Subnuclear Sequestration. *Cell Reports*. 3: 671–677.

Kim, Y., Yeom, M., Kim, H., Lim, J., Koo, H.J., Hwang, D., et al. (2012) GIGANTEA and EARLY FLOWERING 4 in arabidopsis exhibit differential phase-specific genetic influences over a diurnal cycle. *Molecular Plant*. 5.

Krahmer, J., Goralogia, G.S., Kubota, A., Zardilis, A., Johnson, R.S., Song, Y.H., et al. (2019) Time-resolved interaction proteomics of the GIGANTEA protein under diurnal cycles in Arabidopsis. *FEBS Letters*. 593: 319–338.

Kubota, A., Ito, S., Shim, J.S., Johnson, R.S., Song, Y.H., Breton, G., et al. (2017) TCP4-dependent induction of CONSTANS transcription requires GIGANTEA in photoperiodic flowering in Arabidopsis. *PLoS Genetics*. 13: e1006856.

Kurepa, J., Smalle, J., Van Montagu, M., Inze, D., and Inzé, D. (1998) Oxidative stress tolerance and longevity in arabidopsis: The late-flowering mutant gigantea is tolerant to paraquat. *Plant J*. 14: 759–764.

Lång, V., and Palva, E.T. (1992) The expression of a rab-related gene, rab18, is induced by abscisic acid during the cold acclimation process of Arabidopsis thaliana (L.) Heynh. *Plant Molecular Biology*. 20: 951–962.

Langmead, B., and Salzberg, S.L. (2012) Fast gapped-read alignment with Bowtie 2. *Nature Methods*. 9: 357–359.

Laubinger, S., Marchal, V., Gentillhomme, J., Wenkel, S., Adrian, J., Jang, S., et al. (2006) Arabidopsis SPA proteins regulate photoperiodic flowering and interact with the floral inducer CONSTANS to regulate its stability. *Development*. 133: 3213–3222.

Lee, H.G., Mas, P., and Seo, P.J. (2016) MYB96 shapes the circadian gating of ABA signaling in Arabidopsis. *Scientific Reports*. 6: 17754.

Legnaioli, T., Cuevas, J., and Mas, P. (2009) TOC1 functions as a molecular switch connecting the circadian clock with plant responses to drought. *EMBO Journal*. 28: 3745–3757.

Leivar, P., and Monte, E. (2014) PIFs: Systems integrators in plant development. *Plant Cell*. 26: 56–78.

Leung, J., Merlot, S., and Giraudat, J. (1997) The arabidopsis ABSCISIC ACID-INSENSITIVE2 (ABI2) and ABI1 genes encode homologous protein phosphatases 2C involved in abscisic acid signal transduction. *Plant Cell*. 9: 759–771.

Li, B., and Dewey, C.N. (2011) RSEM: Accurate transcript quantification from RNA-Seq data with or without a reference genome. *BMC Bioinformatics*. 12.
Lopez-Molina, L. (2003) AFP is a novel negative regulator of ABA signaling that promotes ABI5 protein degradation. *Genes & Development*. 17: 410–418.
Ma, Y., Szostkiewicz, I., Korte, A., Moes, D., Yang, Y., Christmann, A., et al. (2009) Regulators of PP2C Phosphatase Activity Function as Abscisic Acid Sensors. *Science (1979)*. 324: 1064–8.
Martin-Tryon, E.L., Kreps, J.A., and Harmer, S.L. (2007) GIGANTEA Acts in Blue Light Signaling and Has Biochemically Separable Roles in Circadian Clock and Flowering Time Regulation. *Plant Physiology*. 143: 473–486.
Minkoff, B.B., Stecker, K.E., and Sussman, M.R. (2015) Rapid Phosphoproteomic Effects of Abscisic Acid (ABA) on Wild-Type and ABA Receptor-Deficient A. thaliana Mutants. *Mol Cell Proteomics*. 14: 1169–82.
Mishra, P., and Panigrahi, K.C. (2015) GIGANTEA - an emerging story. *Frontiers in Plant Science*. 6: 1–15.
Mitula, F., Tajdel, M., Ciešla, A., Kasprowicz-Maluški, A., Kulik, A., Babula-Skowrońska, D., et al. (2015) Arabidopsis ABA-Activated Kinase MAPKKK18 is Regulated by Protein Phosphatase 2C ABI1 and the Ubiquitin-Proteasome Pathway. *Plant and Cell Physiology*. 56: 2351–2367.
Miyazono, K.I., Miyakawa, T., Sawano, Y., Kubota, K., Kang, H.J., Asano, A., et al. (2009) Structural basis of abscisic acid signalling. *Nature*. 462: 609–614.
Mizoguchi, T., Wright, L., Fujiwara, S., Cremer, F., Lee, K., Onouchi, H., et al. (2005) Distinct Roles of GIGANTEA in Promoting Flowering and Regulating Circadian Rhythms in Arabidopsis. *The Plant Cell*. 17: 2255–2270.
Mizuno, T., and Yamashino, T. (2008) Comparative Transcriptome of Diurnally Oscillating Genes and Hormone-Responsive Genes in Arabidopsis thaliana: Insight into Circadian Clock-Controlled Daily Responses to Common Ambient Stresses in Plants. *Plant and Cell Physiology*. 49: 481–487.
Mugford, S.T., Fernandez, O., Brinton, J., Flis, A., Krohn, N., Encke, B., et al. (2014) Regulatory properties of ADP glucose pyrophosphorylase are required for adjustment of leaf starch synthesis in different photoperiods. *Plant Physiology*. 166: 1733–1747.
Munemasa, S., Hauser, F., Park, J., Waadt, R., Brandt, B., and Schroeder, J.I. (2015) Mechanisms of abscisic acid-mediated control of stomatal aperture. *Current Opinion in Plant Biology*. 28: 154–162.
Nakamichi, N., Takao, S., Kudo, T., Kiba, T., Wang, Y., Kinoshita, T., et al. (2016) Improvement of Arabidopsis Biomass and Cold, Drought and Salinity Stress Tolerance by Modified Circadian Clock-Associated PSEUDO-RESPONSE REGULATORs. *Plant and Cell Physiology*. 57: 1085–1097.
Niyogi, K.K., Grossman, A.R., and Björkman, O. (1998) Arabidopsis mutants define a central role for the xanthophyll cycle in the regulation of photosynthetic energy conversion. *Plant Cell*. 10: 1121–1134.
Nohales, M.A., Liu, W., Duffy, T., Nozue, K., Sawa, M., Pruneda-Paz, J.L., et al. (2019) Multi-level Modulation of Light Signaling by GIGANTEA Regulates Both the Output and Pace of the Circadian Clock. *Developmental Cell*. 49: 840-851.e8.

Park, D.H., Somers, D.E., Kim, Y.S., Choy, Y.H., Lim, H.K., Soh, M.S., et al. (1999) Control of circadian rhythms and photoperiodic flowering by the Arabidopsis GIGANTEA gene. *Science (1979)*. 285: 1579–1582.

Park, S.-Y., Fung, P., Nishimura, N., Jensen, D.R., Fujii, H., Zhao, Y., et al. (2009) Abscisic Acid Inhibits Type 2C Protein Phosphatases via the PYR/PYL Family of START Proteins. *Science (1979)*. 324: 1068–71.

Pfeiffer, A., Shi, H., Tepperman, J.M., Zhang, Y., and Quail, P.H. (2014) Combinatorial complexity in a transcriptionally centered signaling hub in arabidopsis. *Molecular Plant*. 7: 1598–1618.

Raivo, K. (2012) Pheatmap: pretty heatmaps. *R Pacakage Version*. 61: 915.

Riboni, M., Galbiati, M., Tonelli, C., and Conti, L. (2013) GIGANTEA enables drought escape response via abscisic acid-dependent activation of the florigens and SUPPRESSOR of OVEREXPRESSION of CONSTANS11[c][w]. *Plant Physiology*. 162: 1706–1719.

Riboni, M., Test, A.R., Galbiati, M., Tonelli, C., and Conti, L. (2016) ABA-dependent control of GIGANTEA signalling enables drought escape via up-regulation of FLOWERING LOCUS T in Arabidopsis thaliana. *Journal of Experimental Botany*. 67: 6309–6322.

Robinson, M.D., McCarthy, D.J., and Smyth, G.K. (2009) edgeR: A Bioconductor package for differential expression analysis of digital gene expression data. *Bioinformatics*. 26: 139–140.

Rock, C.D., and Zeevaart, J.A.D. (1991) The aba mutant of Arabidopsis thaliana is impaired in epoxy-carotenoid biosynthesis. *Proc Natl Acad Sci U S A*. 88: 7496–7499.

Rubio, S., Rodrigues, A., Saez, A., Dizon, M.B., Galle, A., Kim, T.-H., et al. (2009) Triple Loss of Function of Protein Phosphatases Type 2C Leads to Partial Constitutive Response to Endogenous Abscisic Acid. *Plant Physiology*. 150: 1345–1355.

Salem, M.A., Yoshida, T., Perez de Souza, L., Alseekh, S., Bajdzienko, K., Fernie, A.R., et al. (2020) An improved extraction method enables the comprehensive analysis of lipids, proteins, metabolites and phytohormones from a single sample of leaf tissue under water-deficit stress. *Plant Journal*. 103: 1614–1632.

Santiago, J., Dupeux, F., Round, A., Antoni, R., Park, S.Y., Jamin, M., et al. (2009) The abscisic acid receptor PYR1 in complex with abscisic acid. *Nature*. 462: 665–668.

Sawa, M., and Kay, S.A. (2011) GIGANTEA directly activates Flowering Locus T in Arabidopsis thaliana. *Proceedings of the National Academy of Sciences*. 108: 11698–11703.

Sawa, M., Nusinow, D.A., Kay, S.A., and Imaizumi, T. (2007) FKF1 and GIGANTEA Complex Formation Is Required for Day-Length Measurement in Arabidopsis. *Science (1979)*. 318: 261–265.

Seung, D., Risopatron, J.P.M., Jones, B.J., and Marc, J. (2012) Circadian clock-dependent gating in ABA signalling networks. *Protoplasma*. 249: 445–457.

Simon, N.M.L., Graham, C.A., Comben, N.E., Hetherington, A.M., and Dodd, A.N. (2020) The circadian clock influences the long-term water use efficiency of Arabidopsis1[open]. *Plant Physiology*. 183: 317–330.

Song, L., Huang, S.S.C., Wise, A., Castanoz, R., Nery, J.R., Chen, H., et al. (2016) A transcription factor hierarchy defines an environmental stress response network. *Science (1979)*. 354: aag1550–aag1550.

Umezawa, T., Sugiyama, N., Mizoguchi, M., Hayashi, S., Myouga, F., Yamaguchi-Shinozaki, K., et al. (2009) Type 2C protein phosphatases directly regulate abscisic acid-activated protein kinases in Arabidopsis. *Proc Natl Acad Sci U S A*. 106: 17588–17593.

Umezawa, T., Sugiyama, N., Takahashi, F., Anderson, J.C., Ishihama, Y., Peck, S.C., et al. (2013) Genetics and phosphoproteomics reveal a protein phosphorylation network in the abscisic acid signaling pathway in arabidopsis thaliana. *Science Signaling*. 6: rs8.

Vlad, F., Rubio, S., Rodrigues, A., Sirichandra, C., Belin, C., Robert, N., et al. (2009) Protein phosphatases 2C regulate the activation of the Snf1-related kinase OST1 by abscisic acid in Arabidopsis. *Plant Cell*. 21: 3170–3184.

Vlieghe, D., Sandelin, A., De Bleser, P.J., Vleminckx, K., Wasserman, W.W., van Roy, F., et al. (2006) A new generation of JASPAR, the open-access repository for transcription factor binding site profiles. *Nucleic Acids Res*. 34.

Wang, P., Xue, L., Batelli, G., Lee, S., Hou, Y.J., Van Oosten, M.J., et al. (2013) Quantitative phosphoproteomics identifies SnRK2 protein kinase substrates and reveals the effectors of abscisic acid action. *Proc Natl Acad Sci U S A*. 110: 11205–11210.

Wang, X., Guo, C., Peng, J., Li, C., Wan, F., Zhang, S., et al. (2019) ABRE-BINDING FACTORS play a role in the feedback regulation of ABA signaling by mediating rapid ABA induction of ABA co-receptor genes. *New Phytologist*. 221: 341–355.

Wickham, H. (2016) ggplot2, Use R! Springer International Publishing, Cham.

Yang, Z., Liu, J., Tischer, S. V., Christmann, A., Windisch, W., Schnyder, H., et al. (2016) Leveraging abscisic acid receptors for efficient water use in Arabidopsis. *Proc Natl Acad Sci U S A*. 113: 6791–6796.

Yoshida, T., Fujita, Y., Maruyama, K., Mogami, J., Todaka, D., Shinozaki, K., et al. (2015) Four Arabidopsis AREB/ABF transcription factors function predominantly in gene expression downstream of SnRK2 kinases in abscisic acid signalling in response to osmotic stress. *Plant, Cell and Environment*. 38: 35–49.

Yu, J.-W., Rubio, V., Lee, N.-Y., Bai, S., Lee, S.-Y., Kim, S.-S., et al. (2008) COP1 and ELF3 Control Circadian Function and Photoperiodic Flowering by Regulating GI Stability. *Molecular Cell*. 32: 617–630.

Zambelli, F., Pesole, G., and Pavesi, G. (2009) Pscan: Finding over-represented transcription factor binding site motifs in sequences from co-regulated or co-expressed genes. *Nucleic Acids Research*. 37.

Legends to Figures

Figure 1. Strong contribution of time of the day in the regulation of drought responses.

(A) Schematic representation of the experimental design. Samples for RNA-seq were harvested at the indicated time points (ZT1 to ZT16) in the light phase encompassing the transition from the last short day and the first long day (photo-extension).

(B) Pyramid plots showing numbers of up-regulated and down-regulated DEGs in the comparison of water deficit vs. well-watered conditions (dubbed as treatment and control, respectively) in the wild type at matched time-points (ZT1 to ZT16). Right (blue) and left (red) bars represent upregulated or downregulated genes, respectively.

(C) Heatmap illustrates the total number of DEGs in response to water deficit in the wild type from ZT1 to ZT16. Colours indicate the overlap (%) for each pairwise comparison according to the colour scale positioned on the right. The horizontal bar chart on the right represents the total number of DEGs detected at each ZT/condition combination (grey) and those which are in common with any the other ZTs/conditions (black).

(D) PCA analyses of DEGs (n = 4780). The same plot is shown in three panels with different colour codes to highlight the genotype, time points and treatment (left to right). Each dot represents one biological replicate.

Figure 2. RNA-seq analysis of GI and ABA regulated genes reveals a phase of ABA insensitivity regulated by GI.

(A, B) Pyramid plots showing numbers of up-regulated and down-regulated DEGs in the comparison of *gi-2* vs. wild type at matched time-points (ZT1 to ZT16) under control (A) or water deficit conditions (B). Right (blue) and left (red) bars represent upregulated or downregulated genes, respectively.

(C) Heatmap displaying the total number of DEGs in *gi-2* compared with the wild type at ZT1 and ZT12 under different irrigation schemes. Colours indicate the overlap (%) for each pairwise comparison according to the colour scale positioned on the right. The horizontal bar chart on the right represents the total number of DEGs detected at each ZT/condition combination (grey) and those which are in common with any the other ZTs/conditions (black).

(D) Boxplot of the distribution of log2(Fold Change) of DEGs between *gi-2* and wild-type plants under water deficit, at ZT12 in (from left to right); wild type water

deficit vs. control condition; *gi-2* water deficit vs. control condition; *gi-2* vs. wild type under water deficit. Genes upregulated in the comparison between *gi-2* and the wild type under water deficit are represented in blue, downregulated genes are represented in red.

Figure 3. Enrichment of PIFs, ABFs and GI binding at GI/ABA DEGs

(A) Heatmap of the statistically significant (FDR < = 1e-2 in at least one comparison) enriched transcription factor binding sites at the ABA and GI DEGs at ZT1 and ZT12 time points under control or water deficit conditions. See Table S2 for a complete list.

(B) Pyramid plot showing number of up-regulated and downregulated DEGs in each comparison and their overlap with PIFs and ABFs ChIP-seq peaks. The following datasets - PIF4, GEO: GSE43284, GSE68193, GSE35315, PIF3, GEO: GSE39215, PIF1, GEO: GSE43283, PIF5, GEO: GSE35059, GSE68193 - were pooled to identify potential target of the PIF family of transcription factors. Similarly, candidate target genes of ABFs were obtained by pooling GBF3, GBF2, ABF1, ABF4 (GEO: GSE80564) datasets, with no regard to experiment conditions (ABA treatment, EtOH treatment). Colour code represents binding to individual or both classes of transcription factors.

(C) Pyramid plot showing the overlap between GI ChIP-seq peaks (SD ZT8) and DEGs obtained in this study. *gi-2* vs. WT (top), *aba1-6* vs. WT (bottom). Asterisks in (A) and (B) are used to indicate a statistically significant over-representation of up regulated genes based on Fisher's exact test.

Figure 4. Deregulation of ABA signalling genes in *gi-2* mutants

(A) and (B) Volcano plots showing a selection of ABA/Cold and circadian-related DEGs in *gi-2* (top) or *aba1-6* mutants (bottom panel) at ZT12 under water deficit. LogFC is reported on the X-axis. FDR on the Y axis. Differentially expressed genes (FDR for differential expression <= 0.05) are represented in purple, non-differentially expressed genes (FDR > 0.05) in green. Selected genes are displayed in yellow. See also Fig. S4 for ZT1 analysis.

Figure 5. GI controls daytime variations in transpiration.

(A) Thermogram of representative plants grown under SDs under well-watered conditions and then sprayed with ABA (or mock) before shifting to LDs. Plants were

grown in separate pots and photographed for thermal imaging on the second LD at the indicated time points.

(B) Leaf temperature data extracted from images shown in (A). n = 5-7 biological replicates per genotype. Values for each genotype / condition combination represent the mean and associated SD. Asterisks indicate statistically significant effect (*p<0.05, **P<0.01, ***P<0.001 and **** p<0.0001) for the genotype (Geno). A detected statistically significant Genotype X Treatment effect (G X T) is show for ZT8.

(C) Simplified model of the GI regulatory role of water deficit responses. GI protein levels increase during the day (blue dotted line) reaching a peak at approx. ZT8. Peak GI expression and function contribute to reducing ABA-depended responses, perhaps to counteract increasing ABA levels (red dotted line). GI may interfere with TFs functions (e.g., the ABFs and the PIFs) for the activation of ABA signalling and optimise plant growth performances under water deficit.

Figure 1

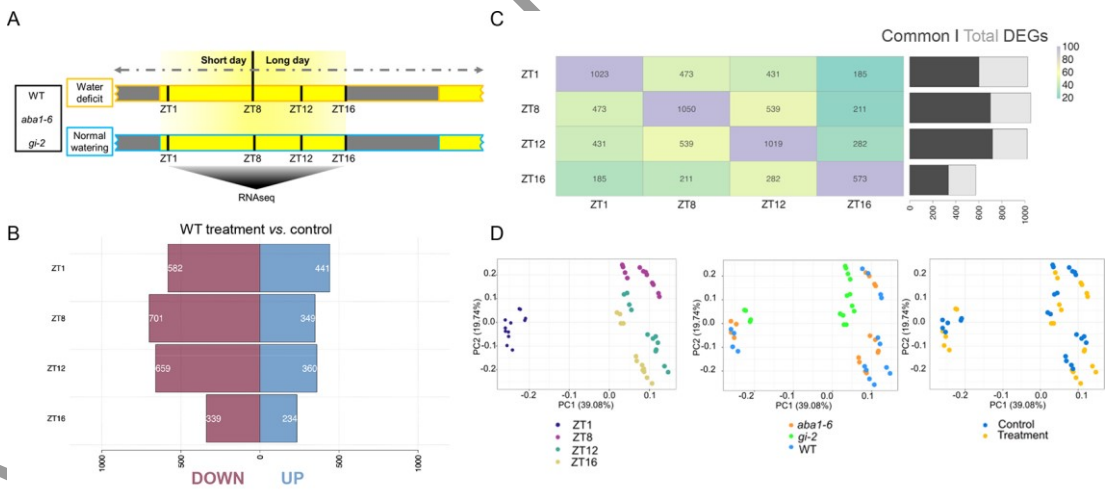

Figure 1

Figure 2

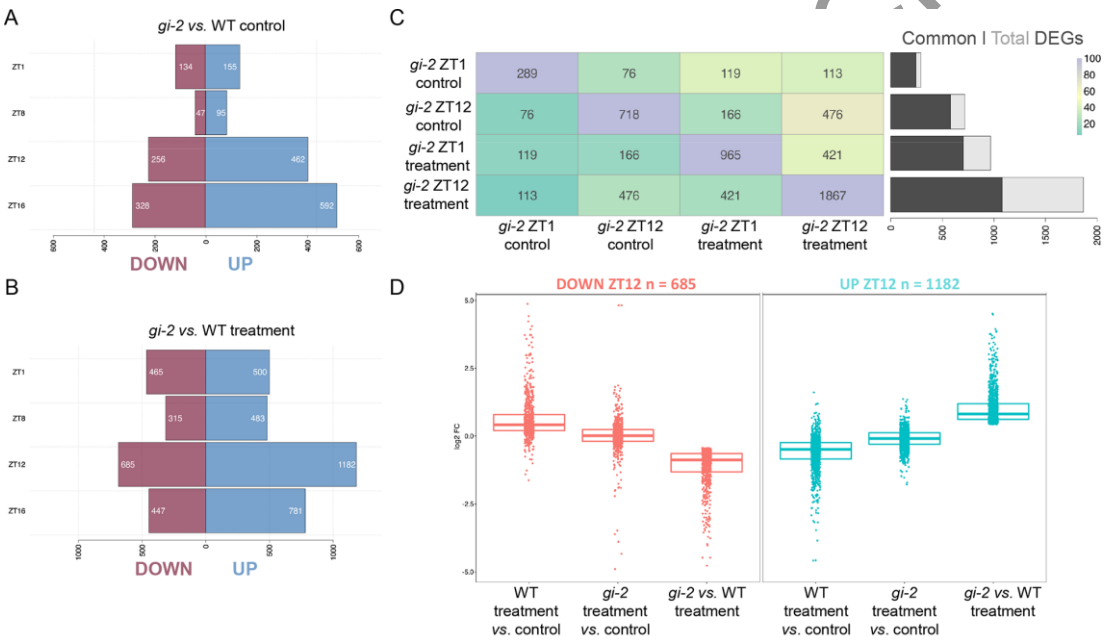

Figure 2

Figure 3

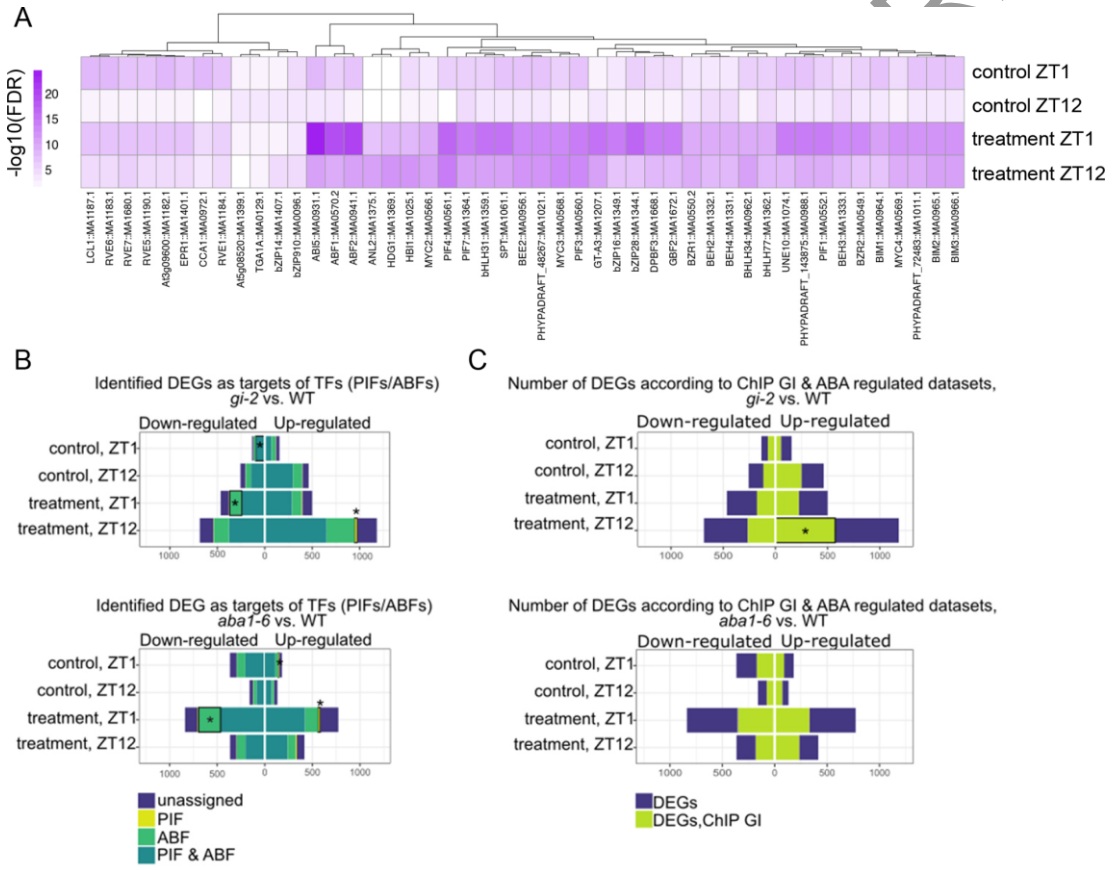

Figure 3

Figure 4

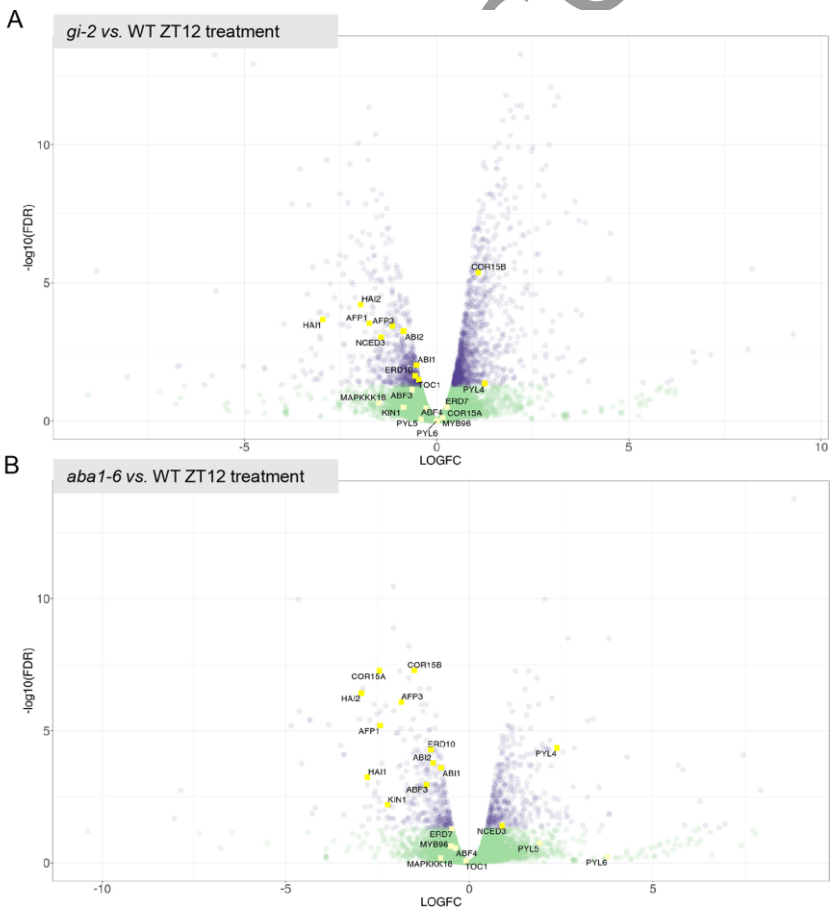

Figure 4

Figure 5

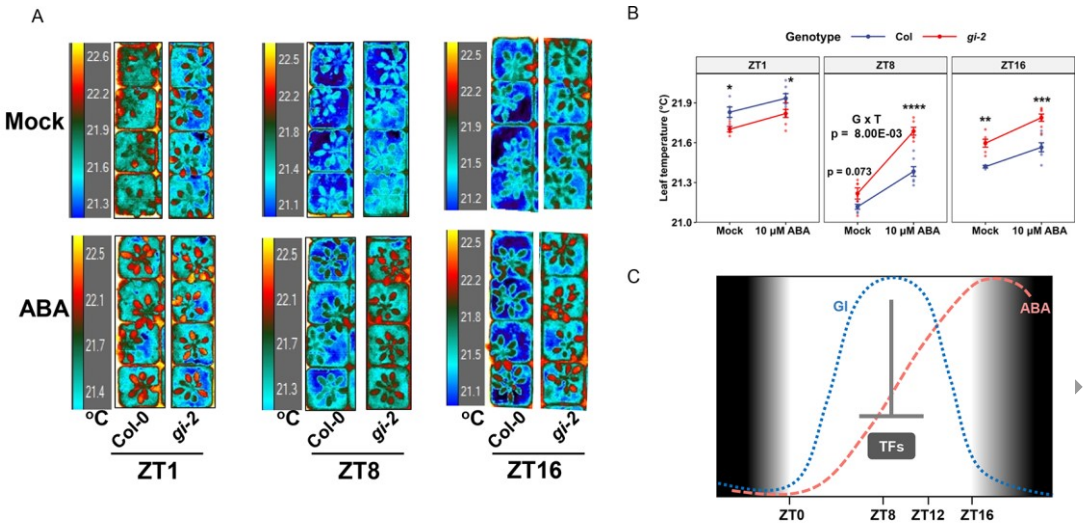

Figure 5